Determining key upstream rainout and convection zones affecting δ18O in water vapor and precipitation based on 8-year continuous observations in the East Asian Monsoon region

Zhaojun Zhan
Nanjing University https://orcid.org/0000-0003-0586-7474
Hongxi Pang (hxpang@nju.edu.cn)
Nanjing University
Shuangye Wu
University of Dayton
Zhengyu Liu
The Ohio State University https://orcid.org/0000-0003-4554-2666
Wangbin Zhang
Nanjing University
Tao Xu
Nanjing University
Hui Liu
Nanjing University
Shugui Hou
Shanghai Jiao Tong University

Article

Keywords: rainout, convection zones, East Asian Monsoon region

Posted Date: May 19th, 2021

DOI: https://doi.org/10.21203/rs.3.rs-493026/v1

Determining key upstream rainout and convection zones affecting $\delta^{18}O$ in water vapor and precipitation based on 8-year continuous observations in the East Asian Monsoon region

Zhaojun Zhan[a], Hongxi Pang[a,b*], Shuangye Wu[c], Zhengyu Liu[d], Wangbin Zhang[a], Tao Xu[a], Hui Liu[a], and Shugui Hou[a,b,e*]

[a] Key Laboratory of Coast and Island Development of Ministry of Education, School of Geography and Ocean Science, Nanjing University, Nanjing, China.

[b] Collaborative Innovation Center of Climate Change, Jiangsu Province Nanjing, China

[c] Department of Geology, University of Dayton, Dayton, OH, USA

[d] Department of Geography, The Ohio State University, Columbus, OH, USA

[e] School of Oceanography, Shanghai Jiao Tong University, Shanghai, China

*Corresponding author: S. Hou (shuguihou@sjtu.edu.cn) and H. Pang (hxpang@nju.edu.cn)

Abstract

More and more studies have recognized the crucial impact of upstream rainout effect and convective activities on the stable isotopic composition of precipitation ($\delta^{18}O_p$) and water vapor ($\delta^{18}O_v$) at mid and low latitudes. However, it is difficult to precisely identify the upstream rainout and convection zones using the traditional time-lagged spatial correlation method. Based on a continuous high-resolution $\delta^{18}O_v$ and $\delta^{18}O_p$ dataset in Nanjing (eastern China), a novel method of upstream key rainout region identification (UKRRI) is developed for reliably identifying the key upstream rainout and convection zones. Based on the UKRRI method, we find that summer $\delta^{18}O_v$ and $\delta^{18}O_p$ in Nanjing are primarily controlled by the rainout effect and convective activities along the moisture transport pathway from the Maritime Continent (MC), via the Indo-China Peninsula and South China Sea (ICP_SCS), to Southeastern China (SEC), particularly over SEC. Contrary to existing studies, the Indian Ocean is not a major rainout and convection zone affecting $\delta^{18}O_p$ and $\delta^{18}O_v$ in Nanjing. Our study has significant implications for the interpretation of stalagmite $\delta^{18}O$ records in East Asian Monsoon (EAM) region.

Introduction

The amount effect refers to the negative correlation between monthly precipitation isotopic composition ($\delta^{18}O_p$) and monthly rainfall amount observed in low latitudes[1]. It is the theoretical basis for the paleoclimate reconstruction from stable isotopic records of stalagmites, ice cores and tree rings in monsoon regions. However, the amount effect

has been questioned by precipitation isotope observations at event[2], daily[3], monthly[4] and inter-annual[5] timescales, causing intense debate on the interpretation of isotopic records from paleoclimate proxies in the East Asian Monsoon (EAM) region[6].

Asian speleothem $\delta^{18}O$ records have been interpreted as “rainfall amount”[7-9] and “monsoon intensity”[10-13]. Other processes are also emphasized, such as changes in atmospheric-ocean circulation (variation of moisture sources)[5, 14], and the integrated regional precipitation variation from moisture sources to cave site[15]. In general, $\delta^{18}O$ records in speleothem have inherited the isotopic signal of precipitation, assuming deposition under equilibrium conditions[10, 16-17]. Thus, there is an urgent need to understand the precise controlling factors for modern $\delta^{18}O_p$, which becomes possible with the development of laser spectroscopic technologies[18-20] and the subsequent availability of continuous high-resolution observations of both precipitation and water vapor isotopic composition ($\delta^{18}O_p$ and $\delta^{18}O_v$). Numerous studies found that variation of $\delta^{18}O_p$ and $\delta^{18}O_v$ in rainy seasons are primarily controlled by upstream rainout process and large-scale convective activities, rather than local meteorological conditions, in mid and low latitude regions such as the Asian Monsoon region[21-26], Indian Monsoon region[27-29], tropical oceans[30-34], Australian Monsoon region[35], Central and South America[36-40], and African Monsoon region[41-42] (more details are summarized in Fig. 1 and Supplementary Table 1).

Most of these studies used the time-lagged spatial correlation analysis between stable isotopes ($\delta^{18}O_p$, $\delta^{18}O_v$) and convective index (such as Outgoing Longwave Radiation, OLR), and identified the key upstream rainout and convection zone as the region with the highest correlation coefficients for a lead time of *N* days. Nevertheless, there are several problems with this method. First, most of spatial correlation analyses did not consider the actual moisture transport pathways[2, 43-44]. Second, even though some studies calculated the time-lagged correlation between $\delta^{18}O_p$ and the cumulative precipitation along air mass back trajectories[21, 24, 35, 45], they did not consider the time difference among moisture transport from different source regions. As a result, the high correlation areas identified in these studies could result from atmospheric teleconnections and other spurious correlations[46].

In light of such methodological issues, a more reliable method is desirable to better identify the upstream rainout and convection zones. This requires long-term, high-resolution stable isotope observations. Benefit from the laser spectroscopic techniques, high-resolution $\delta^{18}O_p$ and $\delta^{18}O_v$ data have been collected for many sites during the past decade, but few of them offer continuous long-term observations (Supplementary Table 1). In this study, we use an 8-year continuous high-resolution $\delta^{18}O_p$ and $\delta^{18}O_v$ dataset for Nanjing (southeastern China) to develop a better method for identifying key upstream rainout and convection zones affecting Nanjing $\delta^{18}O_p$ and $\delta^{18}O_v$ in the summer monsoon seasons (June-September, JJAS). Our results highlight the crucial importance of rainout processes and convective activities along the moisture transport pathways, and provide a new perspective for the interpretation of stalagmite $\delta^{18}O$ records in the EAM region.

Isotopic observations of water vapor and precipitation

We established the atmospheric water vapor isotope observation system (Picarro L2120-i wavelength scanned cavity ring down spectroscopy, WS-CRDS) in the Station for Observing Regional Processes of the Earth System at Nanjing University (SORPES-NJU) (32.12°N, 118.95°E)[47], and started the $\delta^{18}O_v$ data collection from 1st November 2012. It continues to present, but the dataset used in this study ends on 30 September, 2019. More details on the water vapor sampling and analysis procedures can be found in Li et al. (2020)[48]. We measured two reference standard liquid samples for data calibration: SD1 ($\delta^{18}O$ of -10.009‰, δD of -69.476‰) and SD2 ($\delta^{18}O$ of -29.676‰, δD of -225.372‰), provided by the Key Laboratory of Coast and Island Development of the Ministry of Education. In order to eliminate the influence of concentration dependency and drift of the isotopic composition during measurements[49-50], detailed calibration were carried out for the in-situ measurement data[48, 51]. The final $\delta^{18}O_v$ data was standardized to the IAEA VSMOW2-SLAP2 scale and averaged into daily data for this study. The analytical uncertainty was less than 0.2‰ for $\delta^{18}O_v$ and 1‰ for δD_v[48, 51].

Precipitation samples were collected on rainy days from September 2011 to present, and the data used in this study ends in September 2019. Samples were sealed into 100 mL polyethylene bottles and frozen at approximately -2°C before measurement. Precipitation samples were measured by a Picarro L2120-i system, with the measurement precision less than 0.1‰ for $\delta^{18}O_p$ and 0.5‰ for δD_p. More details on the analysis procedures were outlined in Tang et al. (2015)[25].

A novel method for identifying upstream rainout and convection zones

As mentioned above, the existing spatial correlation method failed to consider the real moisture transport paths, and account for the time difference in moisture transport from different source regions. To counter these problems, we developed a novel method for more reliable identification of the upstream rainout and convection zones that most impact $\delta^{18}O_p$ and $\delta^{18}O_v$ in Nanjing. OLR was adopted as an indicator of convection[52]. We name the new method as "upstream key rainout region identification (UKRRI)", and Figure 2 provides a flow chart for the UKRRI method, which involves the following three steps.

First, we quantitatively identified the moisture transport paths for all summer precipitation events in Nanjing. This was done by running the HYSPLIT backward trajectory simulation at four initial heights (1000 m, 1500 m, 2000 m and 3000 m) from September 2011 to September 2019. Based on the HYSPLT results, we further identified all moisture uptake locations on precipitating backward trajectories and estimated their contributions (S_p) to precipitation in destination (Nanjing) at the initial trajectory height, utilizing the moisture source diagnostic method outlined in[53].

Second, based on the spatial distribution of moisture uptake locations and regional geographic units, we divided the region into seven moisture source areas: Western Indian Ocean (WIO), Eastern Indian Ocean (EIO), Maritime Continent (MC), Indo-

China Peninsula and South China Sea (ICP_SCS), Western Pacific Ocean (WPO), Southeastern China (SEC), and Northern Continent (NC) (Fig. 3 and Supplementary Table 2). To account for the transport time difference for moisture uptake locations, we extracted each of their OLR value at the exact time when the uptake occurs. For each precipitation event, we calculated the amount (S_p) weighted mean OLR for all moisture uptake locations that fall within each of the seven source regions.

Finally, we calculated the correlation between Nanjing stable isotopes ($\delta^{18}O_p$ and $\delta^{18}O_v$) in summer rainy days and the amount-weighted mean OLR for moisture uptake locations in each moisture source region. According to the correlation results, we can identify the most important upstream rainout and convection zones. In general, this new method effectively takes into account both the moisture transport pathways and the specific lead-time of moisture uptake locations along pathways (Fig. 3), hence provide more accurate results. More details about the UKRRI method can be found in Supplementary Information 2.

Based on the UKRRI method, we also calculated the moisture contribution from each of the seven regions to Nanjing precipitation (Fig. 4), and the average moisture transport time from different source regions (Fig. 3). The great disparity in moisture transport time from different regions further illustrated the necessity and advantage of the UKRRI method to accurately identify upstream rainout and convection zones that impact downstream precipitation isotopic compositions.

Results

Figure 4 presents the regional moisture contribution, and correlation results between Nanjing $\delta^{18}O$ and OLR for different moisture sources at four different initial back-trajectory heights. Results are also summarized in Supplementary Table 3-4. r_p and r_v are correlation coefficients for $\delta^{18}O_p$-OLR and $\delta^{18}O_v$-OLR respectively. Results show that the main pathway for moisture transport is a corridor of high moisture contribution from MC through ICP_SCS to SEC regions.

Along this pathway, the SEC region contributes most moisture to Nanjing summer precipitation at all heights (32.2% - 37.1%), and has the most significant correlations between $\delta^{18}O$-OLR ($0.30 \leq r_p \leq 0.65$, $p < 0.001$; $0.46 \leq r_v \leq 0.78$, $p < 0.001$). The ICP_SCS region contributes between 13.5% and 25.8% of moisture at various heights. The region has significant $\delta^{18}O_p$-OLR correlations ($0.24 \leq r_p \leq 0.37$, $p < 0.01$) at 1500m-3000m AGL, and significant $\delta^{18}O_v$-OLR correlations ($0.24 \leq r_v \leq 0.32$, $p < 0.05$) at 1000m-2000m AGL. The MC region contributes less moisture (7.2% - 10.7%), but has the second highest $\delta^{18}O$-OLR correlations at 1000m-2000m AGL ($0.42 \leq r_p \leq 0.45$, $p < 0.01$; $0.42 \leq r_v \leq 0.58$, $p < 0.01$).

The WPO region is the second most important source region, contributing 18.2% - 34.6% of the total moisture to Nanjing summer precipitation. The $\delta^{18}O$-OLR correlation varies at different initial heights. It has significant $\delta^{18}O_v$-OLR correlations ($0.24 \leq r_v \leq 0.31$, $p < 0.01$) at 1000m-2000m AGL, and significant $\delta^{18}O_p$-OLR correlation ($r_p = 0.36$, $p < 0.001$) at 1500m AGL. Both WIO and EIO contribute very little moisture to Nanjing

summer precipitation, and have very few significant $\delta^{18}O$-OLR correlation, e.g. $\delta^{18}O$-OLR correlation in EIO at 2000m AGL, the $\delta^{18}O_p$-OLR correlation in WIO at 2000m AGL, and the $\delta^{18}O_v$-OLR correlation in WIO at 3000m AGL.

Discussion

Significant positive $\delta^{18}O$-OLR correlations are observed along the MC-ICP_SCS-SEC moisture transport pathway (especially over SEC) at all four initial back-trajectory heights (Fig. 4). This suggests that summer $\delta^{18}O_p$ and $\delta^{18}O_v$ in Nanjing are primary controlled by rainout and convective activities along this moisture pathway because of its dominant moisture contribution to precipitation (Fig. 4). The particular importance of the SEC region in our result is supported by several studies on tracing moisture sources in Yangtze River Basin (YRB), which emphasize the important contribution of the terrestrial moisture from SEC[54-58]. In addition, the inter-annual variation of monthly precipitation amount-weighted average $\delta^{18}O_p$ in Nanjing in summer monsoon season (June-September) is highly consistent with those records from GNIP stations along the MC-ICP_SCS-SEC moisture transport pathway, such as Guangzhou, Hong Kong, Bangkok, Kuala Lumpur and Changsha (Supplementary Fig. 1). This consistency further confirms the importance of upstream rainout process and convective activities along the MC-ICP_SCS-SEC moisture transport pathway to the variation of summer $\delta^{18}O_p$ and $\delta^{18}O_v$ in Nanjing.

Although the WPO region has significant moisture contributions, it shows lower $\delta^{18}O$-OLR correlations at four initial back-trajectory heights. This suggests that moisture source has only an indirect effect on the stable isotopic composition, the variation of which also depends on whether the air masses go through convection zones[43, 59].

Despite the general belief that moisture transport from the Indian Ocean (IO) is important for the whole monsoon region, the EIO and WIO regions only contribute 2.0% - 6.7% and 0.7% - 2.8% respectively to our study area at 1000m-3000m AGL. Similar results are also found by Shi et al. (2020)[56], who estimates the moisture contribution from IO at only 2.4% ~ 9.5% during four sub-periods of the monsoon season even though it accounts for half of trajectories for YRB. This is largely because of the substantial moisture loss over moisture sink regions (Indian Peninsula and Indochina Peninsula). Consistent with the small moisture contribution from IO, the EIO and WIO regions show very few significant $\delta^{18}O$-OLR correlations in this study (Fig. 4). These results suggest that the Indian Ocean is neither a dominant moisture source, nor a main rainout and convection zone affecting $\delta^{18}O_p$ and $\delta^{18}O_v$ in the EAM region. Our result is contrary to the conclusions of several previous studies in stalagmite $\delta^{18}O$ records and isotope-embedded climate simulations in EAM region, which emphasize the role of upstream processes in the tropical Indian Ocean in depleting precipitation $\delta^{18}O$ in the EAM region[16-17, 60-62]. However, the significance of these processes in Indian Ocean on the EAM stalagmite $\delta^{18}O$ is not supported by the notable difference of stalagmite $\delta^{18}O$ records between the EAM and ISM regions in terms of phase, variation amplitude and pattern on the glacial-interglacial as well as shorter than millennial time scales[13, 63-68]. Therefore, our results could provide a new perspective for interpreting stalagmite $\delta^{18}O$

records in EAM region.

Conclusions

In this study, we develop a novel UKRRI method for identifying the key upstream rainout and convection zones for summer precipitation in Nanjing, taking into account the exact moisture transport pathway and the specific time difference for moisture transport from different source regions. By doing so, it effectively overcame the deficiency of traditional spatial correlation analysis method. Our results indicate that summer $\delta^{18}O_p$ and $\delta^{18}O_v$ in Nanjing are primarily controlled by the rainout effect and convective activities along the moisture transport pathway from the Maritime Continent (MC), via the Indo-China Peninsula and South China Sea (ICP_SCS), to Southeastern China (SEC) (especially over SEC). Contrary to previous studies that emphasized the upstream rainout effect in the tropical Indian Ocean (IO), our results suggest that the IO is neither a dominant moisture source region, nor a major upstream rainout and convection zone affecting summer $\delta^{18}O_p$ and $\delta^{18}O_v$ in Nanjing. Our results could provide a new perspective for interpreting speleothem $\delta^{18}O$ records in the EAM region.

Key upstream rainout and convection zones likely vary for different monsoon regions, because of the differences in topography[43], the distribution of land and sea[38], and large-scale atmosphere circulation[34], etc. This study provides a much needed methodology to use continuous long-term isotopic observation to identify precise upstream rainout and convection zones in global monsoon regions.

Data availability

All isotopic data used in this research are presented with the paper in Supplementary Information 3. Monthly precipitation isotope data from GNIP are available at https://nucleus.iaea.org/wiser. Daily precipitation isotope data at Guangzhou and Changsha are provided by Yang et al. (2018)[69] and Zhou et al. (2019)[24] respectively. The NOAA OLR data (2.5°×2.5°) from the NCEP/NCAR are available at https://www.esrl.noaa.gov/psd/data/gridded/data.interp_OLR.html.

Acknowledgments

This work is supported by the National Natural Science Foundation of China (41771031, 41830644, 91837102, and 42021001), Chinese Arctic and Antarctic Administration (CXPT2020012), the “333 Project” of Jiangsu Province (BRA2020030). We would like to thank the NOAA Air Resource Laboratory (ARL) for providing the HYSPLIT model used in this paper.

Author contributions

S.H. and H.P. developed the essential research idea. Z.Z. collected the precipitation stable isotope data, performed the observation and calibration of water vapor stable isotope data, and wrote the initial draft of this paper. S.W. participated in compiling the code for the novel method in this research, W.B., T.X., and H.L. contributed to the precipitation stable isotope measurement.

Competing financial interests

The authors declare no competing financial interests.

Supplementary materials

Supplementary materials related to this article can be found online at ……

References

1. Dansgaard W. Stable isotopes in precipitation. *Tellus* **16**, 436-468 (1964).
2. He S, Goodkin NF, Jackisch D, Ong MR, Samanta D. Continuous real-time analysis of the isotopic composition of precipitation during tropical rain events: Insights into tropical convection. *Hydrological Processes* **32**, 1531-1545 (2018).
3. Lekshmy PR, Midhun M, Ramesh R, Jani RA. $\delta^{18}O$ depletion in monsoon rain relates to large scale organized convection rather than the amount of rainfall. *Sci Rep* **4**, 5661 (2014).
4. Cai Z, Tian L. Atmospheric Controls on Seasonal and Interannual Variations in the Precipitation Isotope in the East Asian Monsoon Region. *Journal of Climate* **29**, 1339-1352 (2016).
5. Tan M. Circulation effect: response of precipitation $\delta^{18}O$ to the ENSO cycle in monsoon regions of China. *Climate Dynamics* **42**, 1067-1077 (2014).
6. Cheng H, Zhang H, Zhao J, Li H, Ning Y, Kathayat G. Chinese stalagmite paleoclimate researches: A review and perspective. *Science China Earth Sciences* **62**, 1489-1513 (2019).
7. Cai Y*, et al.* Variability of stalagmite-inferred Indian monsoon precipitation over the past 252,000 y. *Proc Natl Acad Sci U S A* **112**, 2954-2959 (2015).
8. Cheng H*, et al.* Ice Age Terminations. *Science* **326**, 248-252 (2009).
9. Wang Y*, et al.* A High-Resolution Absolute-Dated Late Pleistocene Monsoon Record from Hulu Cave, China. *Science* **294**, 2345-2348 (2001).
10. Liu J, Chen J, Zhang X, Li Y, Rao Z, Chen F. Holocene East Asian summer monsoon records in northern China and their inconsistency with Chinese stalagmite $\delta^{18}O$ records. *Earth-Science Reviews* **148**, 194-208 (2015).
11. Wang P*, et al.* Evolution and variability of the Asian monsoon system: state of the art and outstanding issues. *Quaternary Science Reviews* **24**, 595-629 (2005).
12. Yang X*, et al.* Early-Holocene monsoon instability and climatic optimum recorded by Chinese stalagmites. *The Holocene* **29**, 1059-1067 (2019).
13. Zhang H*, et al.* The Asian Summer Monsoon: Teleconnections and Forcing Mechanisms—A Review from Chinese Speleothem $\delta^{18}O$ Records. *Quaternary* **2**, 26 (2019).
14. Maher BA, Thompson R. Oxygen isotopes from Chinese caves: records not of monsoon rainfall but of circulation regime. *Journal of Quaternary Science* **27**, 615-624 (2012).
15. Cheng H*, et al.* The Asian monsoon over the past 640,000 years and ice age terminations. *Nature* **534**, 640-646 (2016).
16. Yang H, Johnson KR, Griffiths ML, Yoshimura K. Interannual controls on oxygen isotope variability in Asian monsoon precipitation and implications for paleoclimate reconstructions. *Journal of Geophysical Research: Atmospheres* **121**, 8410-8428 (2016).
17. Liu ZY*, et al.* Chinese cave records and the East Asia Summer Monsoon. *Quaternary Science Reviews* **83**, 115-128 (2014).
18. Wen X-F, Sun X-M, Zhang S-C, Yu G-R, Sargent SD, Lee X. Continuous measurement of

water vapor D/H and ^{18}O/^{16}O isotope ratios in the atmosphere. *Journal of Hydrology* **349**, 489-500 (2008).

19. Galewsky J, Steen-Larsen HC, Field RD, Worden J, Risi C, Schneider M. Stable isotopes in atmospheric water vapor and applications to the hydrologic cycle. *Reviews of Geophysics* **54**, 809-865 (2016).
20. Crosson E*, et al.* Stable Isotope Ratios Using Cavity Ring-Down Spectroscopy: Determination of ^{13}C/^{12}C for Carbon Dioxide in Human Breath. *Analytical chemistry* **74**, 2003-2007 (2002).
21. Ruan J, Zhang H, Cai Z, Yang X, Yin J. Regional controls on daily to interannual variations of precipitation isotope ratios in Southeast China: Implications for paleomonsoon reconstruction. *Earth and Planetary Science Letters* **527**, 115794 (2019).
22. Dong W*, et al.* Summer rainfall over the southwestern Tibetan Plateau controlled by deep convection over the Indian subcontinent. *Nat Commun* **7**, 10925 (2016).
23. Cai Z, Tian L, Bowen GJ. Spatial-seasonal patterns reveal large-scale atmospheric controls on Asian Monsoon precipitation water isotope ratios. *Earth and Planetary Science Letters* **503**, 158-169 (2018).
24. Zhou H*, et al.* Variation of δ^{18}O in precipitation and its response to upstream atmospheric convection and rainout: A case study of Changsha station, south-central China. *Sci Total Environ* **659**, 1199-1208 (2019).
25. Tang Y, Pang H, Zhang W, Li Y, Wu S, Hou S. Effects of changes in moisture source and the upstream rainout on stable isotopes in precipitation – a case study in Nanjing, eastern China. *Hydrology and Earth System Sciences* **19**, 4293-4306 (2015).
26. Wang Y, Hu C, Ruan J, Johnson KR. East Asian precipitation δ^{18}O relationship with various monsoon indices. *Journal of Geophysical Research: Atmospheres* **125**, e2019JD032282 (2020).
27. Wei Z, Lee X, Liu Z, Seeboonruang U, Koike M, Yoshimura K. Influences of large-scale convection and moisture source on monthly precipitation isotope ratios observed in Thailand, Southeast Asia. *Earth and Planetary Science Letters* **488**, 181-192 (2018).
28. Saranya P, Krishan G, Rao MS, Kumar S, Kumar B. Controls on water vapor isotopes over Roorkee, India: Impact of convective activities and depression systems. *Journal of Hydrology* **557**, 679-687 (2018).
29. Rahul P, Ghosh P. Long term observations on stable isotope ratios in rainwater samples from twin stations over Southern India; identifying the role of amount effect, moisture source and rainout during the dual monsoons. *Climate Dynamics* **52**, 6893-6907 (2019).
30. He S, Goodkin NF, Kurita N, Wang X, Rubin CM. Stable Isotopes of Precipitation During Tropical Sumatra Squalls in Singapore. *Journal of Geophysical Research: Atmospheres* **123**, 3812-3829 (2018).
31. Moerman JW, Cobb KM, Adkins JF, Sodemann H, Clark B, Tuen AA. Diurnal to interannual rainfall δ^{18}O variations in northern Borneo driven by regional hydrology. *Earth and Planetary Science Letters* **369-370**, 108-119 (2013).
32. Lacour J-L, Risi C, Worden J, Clerbaux C, Coheur P-F. Importance of depth and intensity of convection on the isotopic composition of water vapor as seen from IASI and TES δD observations. *Earth and Planetary Science Letters* **481**, 387-394 (2018).
33. Risi C, Bony S, Vimeux F. Influence of convective processes on the isotopic composition

(δ^{18}O and δD) of precipitation and water vapor in the tropics: 2. Physical interpretation of the amount effect. *Journal of Geophysical Research* **113**, D19306 (2008).

34. Permana DS, Thompson LG, Setyadi G. Tropical West Pacific moisture dynamics and climate controls on rainfall isotopic ratios in southern Papua, Indonesia. *Journal of Geophysical Research: Atmospheres* **121**, 2222-2245 (2016).
35. Zwart C, Munksgaard NC, Kurita N, Bird MI. Stable isotopic signature of Australian monsoon controlled by regional convection. *Quaternary Science Reviews* **151**, 228-235 (2016).
36. Villacís M, Vimeux F, Taupin JD. Analysis of the climate controls on the isotopic composition of precipitation (δ^{18}O) at Nuevo Rocafuerte, 74.5°W, 0.9°S, 250 m, Ecuador. *Comptes Rendus Geoscience* **340**, 1-9 (2008).
37. Samuels-Crow KE, Galewsky J, Hardy DR, Sharp ZD, Worden J, Braun C. Upwind convective influences on the isotopic composition of atmospheric water vapor over the tropical Andes. *Journal of Geophysical Research: Atmospheres* **119**, 7051-7063 (2014).
38. Vimeux F, Tremoy G, Risi C, Gallaire R. A strong control of the South American SeeSaw on the intra-seasonal variability of the isotopic composition of precipitation in the Bolivian Andes. *Earth and Planetary Science Letters* **307**, 47-58 (2011).
39. Vimeux F, Gallaire R, Bony S, Hoffmann G, Chiang J. What are the climate controls on δD in precipitation in the Zongo Valley (Bolivia)? Implications for the Illimani ice core interpretation. *Earth and Planetary Science Letters* **240**, 205-220 (2005).
40. Vuille M, Werner M. Stable isotopes in precipitation recording South American summer monsoon and ENSO variability: observations and model results. *Climate Dynamics* **25**, 401-413 (2005).
41. Tremoy G*, et al.* A 1-year long δ^{18}O record of water vapor in Niamey (Niger) reveals insightful atmospheric processes at different timescales. *Geophysical Research Letters* **39**, L08805 (2012).
42. Risi C*, et al.* What controls the isotopic composition of the African monsoon precipitation? Insights from event-based precipitation collected during the 2006 AMMA field campaign. *Geophysical Research Letters* **35**, L24808 (2008).
43. He Y*, et al.* Impact of atmospheric convection on south Tibet summer precipitation isotopologue composition using a combination of in situ measurements, satellite data, and atmospheric general circulation modeling. *Journal of Geophysical Research: Atmospheres* **120**, 3852-3871 (2015).
44. Rahul P, Ghosh P, Bhattacharya SK, Yoshimura K. Controlling factors of rainwater and water vapor isotopes at Bangalore, India: Constraints from observations in 2013 Indian monsoon. *Journal of Geophysical Research: Atmospheres* **121**, 13,936-913,952 (2016).
45. Kurita N. Water isotopic variability in response to mesoscale convective system over the tropical ocean. *Journal of Geophysical Research: Atmospheres* **118**, 10,376-310,390 (2013).
46. Hu J, Emile-Geay J, Partin J. Correlation-based interpretations of paleoclimate data – where statistics meet past climates. *Earth and Planetary Science Letters* **459**, 362-371 (2017).
47. Ding AJ*, et al.* Ozone and fine particle in the western Yangtze River Delta: an overview of 1 yr data at the SORPES station. *Atmospheric Chemistry and Physics* **13**, 5813-5830

(2013).
48. Li Y*, et al.* Variations of Stable Isotopic Composition in Atmospheric Water Vapor and their Controlling Factors—A 6-Year Continuous Sampling Study in Nanjing, Eastern China. *Journal of Geophysical Research: Atmospheres* **125**, e2019JD031697 (2020).
49. Steen-Larsen HC*, et al.* Continuous monitoring of summer surface water vapor isotopic composition above the Greenland Ice Sheet. *Atmospheric Chemistry and Physics* **13**, 4815-4828 (2013).
50. Bailey A, Noone D, Berkelhammer M, Steen-Larsen HC, Sato P. The stability and calibration of water vapor isotope ratio measurements during long-term deployments. *Atmospheric Measurement Techniques* **8**, 4521-4538 (2015).
51. Gu XQ, Pang HX, Li YJ, Zhang WB, Wang JJ. Study on Calibration Method for Atmospheric Water Vapor Stable Isotopes Observed by Cavity Ring-Down Spectroscopy. *Spectroscopy and Spectral Analysis* **39**, 1700-1705 (2019).
52. Wang B, Xu X. Northern Hemisphere Summer Monsoon Singularities and Climatological Intraseasonal Oscillation. *Journal of Climate* **10**, 1071-1085 (1997).
53. Sodemann H, Schwierz C, Wernli H. Interannual variability of Greenland winter precipitation sources: Lagrangian moisture diagnostic and North Atlantic Oscillation influence. *Journal of Geophysical Research* **113**, D03107 (2008).
54. Cheng TF, Lu M. Moisture Source–Receptor Network of the East Asian Summer Monsoon Land Regions and the Associated Atmospheric Steerings. *Journal of Climate* **33**, 9213-9231 (2020).
55. Sun B, Wang H. Analysis of the major atmospheric moisture sources affecting three sub-regions of East China. *International Journal of Climatology* **35**, 2243-2257 (2015).
56. Shi Y, Jiang Z, Liu Z, Li L. A Lagrangian Analysis of Water Vapor Sources and Pathways for Precipitation in East China in Different Stages of the East Asian Summer Monsoon. *Journal of Climate* **33**, 977-992 (2020).
57. Wang N*, et al.* Quantitative diagnosis of moisture sources and transport pathways for summer precipitation over the mid-lower Yangtze River Basin. *Journal of Hydrology* **559**, 252-265 (2018).
58. Wei J, Dirmeyer PA, Bosilovich MG, Wu R. Water vapor sources for Yangtze River Valley rainfall: Climatology, variability, and implications for rainfall forecasting. *Journal of Geophysical Research: Atmospheres* **117**, D05126 (2012).
59. Pang H, Hou S, Kaspari S, Mayewski PA. Influence of regional precipitation patterns on stable isotopes in ice cores from the central Himalayas. *The Cryosphere* **8**, 289-301 (2014).
60. Maher BA. Holocene variability of the East Asian summer monsoon from Chinese cave records: a re-assessment. *The Holocene* **18**, 861-866 (2008).
61. Johnson KR. Long-distance relationship. *Nature Geoscience* **4**, 426-427 (2011).
62. Pausata FSR, Battisti DS, Nisancioglu KH, Bitz CM. Chinese stalagmite $\delta^{18}O$ controlled by changes in the Indian monsoon during a simulated Heinrich event. *Nature Geoscience* **4**, 474-480 (2011).
63. Li D*, et al.* Is Chinese stalagmite $\delta^{18}O$ solely controlled by the Indian summer monsoon? *Climate Dynamics* **53**, 2969-2983 (2019).
64. Hu J, Emile-Geay J, Tabor C, Nusbaumer J, Partin J. Deciphering Oxygen Isotope Records From Chinese Speleothems With an Isotope-Enabled Climate Model. *Paleoceanography*

and Paleoclimatology **34**, 2098-2112 (2019).

65. Sinha A, Berkelhammer M, Stott L, Mudelsee M, Cheng H, Biswas J. The leading mode of Indian Summer Monsoon precipitation variability during the last millennium. *Geophysical Research Letters* **38**, L15703 (2011).
66. Rao Z, Liu X, Hua H, Gao Y, Chen F. Evolving history of the East Asian summer monsoon intensity during the MIS5: inconsistent records from Chinese stalagmites and loess deposits. *Environmental Earth Sciences* **73**, 3937-3950 (2014).
67. Liu G*, et al.* On the glacial-interglacial variability of the Asian monsoon in speleothem $\delta^{18}O$ records. *Sci Adv* **6**, eaay8189 (2020).
68. Tan L*, et al.* Climate significance of speleothem $\delta^{18}O$ from central China on decadal timescale. *Journal of Asian Earth Sciences* **106**, 150-155 (2015).
69. Yang X, Davis ME, Acharya S, Yao T. Asian monsoon variations revealed from stable isotopes in precipitation. *Climate Dynamics* **51**, 2267-2283 (2018).

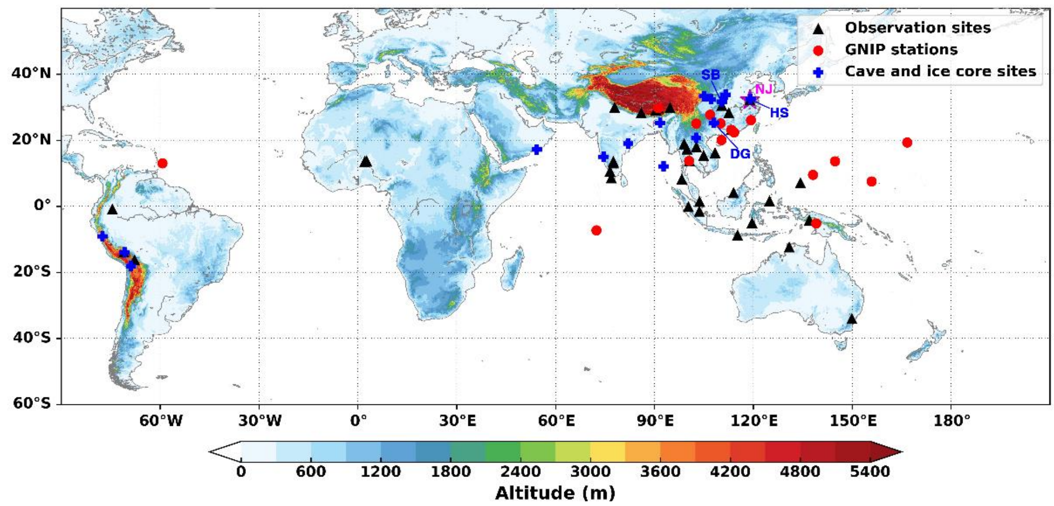

Fig. 1. A map of study sites in global monsoon regions focusing on the effects of upstream rainout and convective activities on precipitation isotopes. Black triangles present the observation sites; red points are GNIP stations from IAEA; and blue crosses are locations of cave speleothem and ice core records in existing studies. The details of these studies are summarized in Supplementary Table 1). The study site of Nanjing is marked by magenta star.

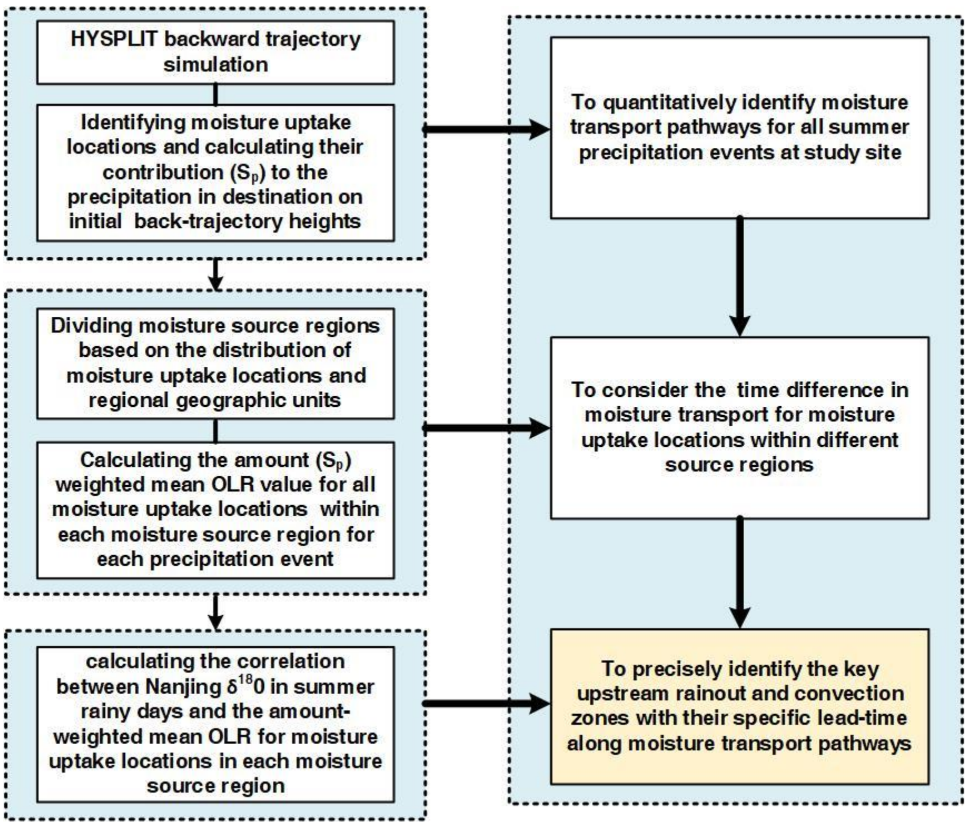

Fig. 2 The flowchart for the UKRRI method for identifying key upstream rainout and convection zones.

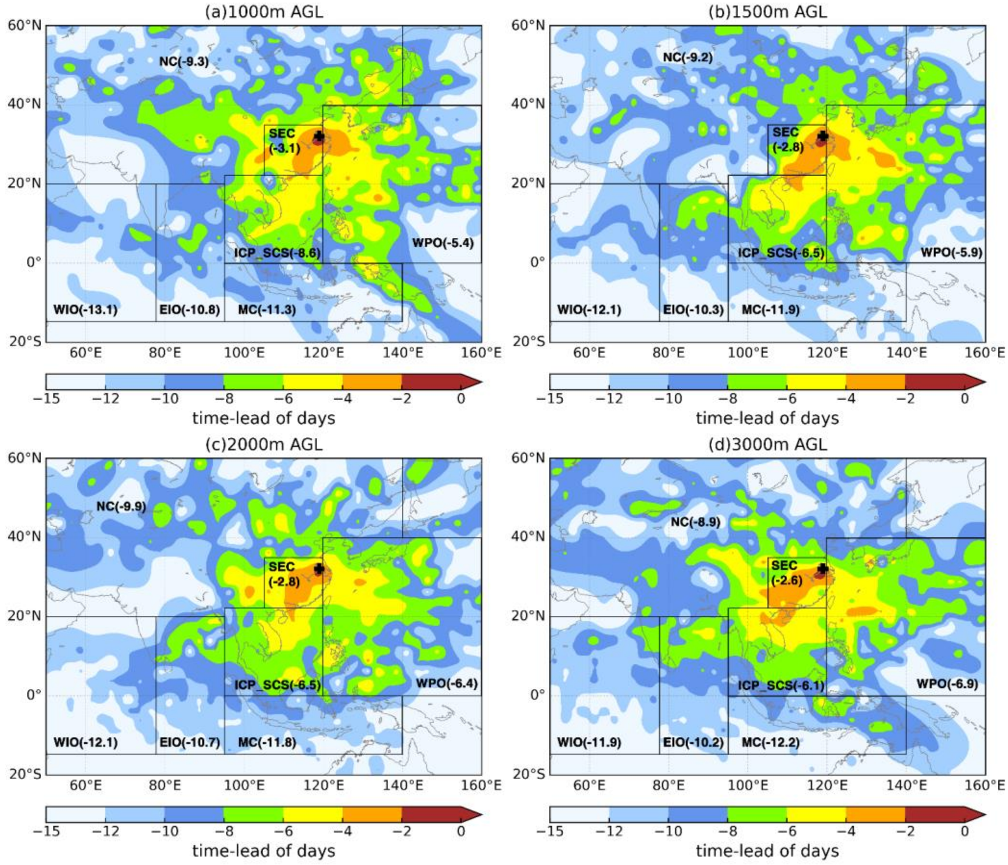

Fig. 3 Moisture transport time (in number of days) to Nanjing at initial back-trajectory heights of 1000m (a), 1500m (b), 2000m (c), and 3000m (d) AGL. The black solid line rectangles represent seven moisture source regions, and the regional average tranport time is presented by the number in black bracket. The study site of Nanjing is marked by a black cross.

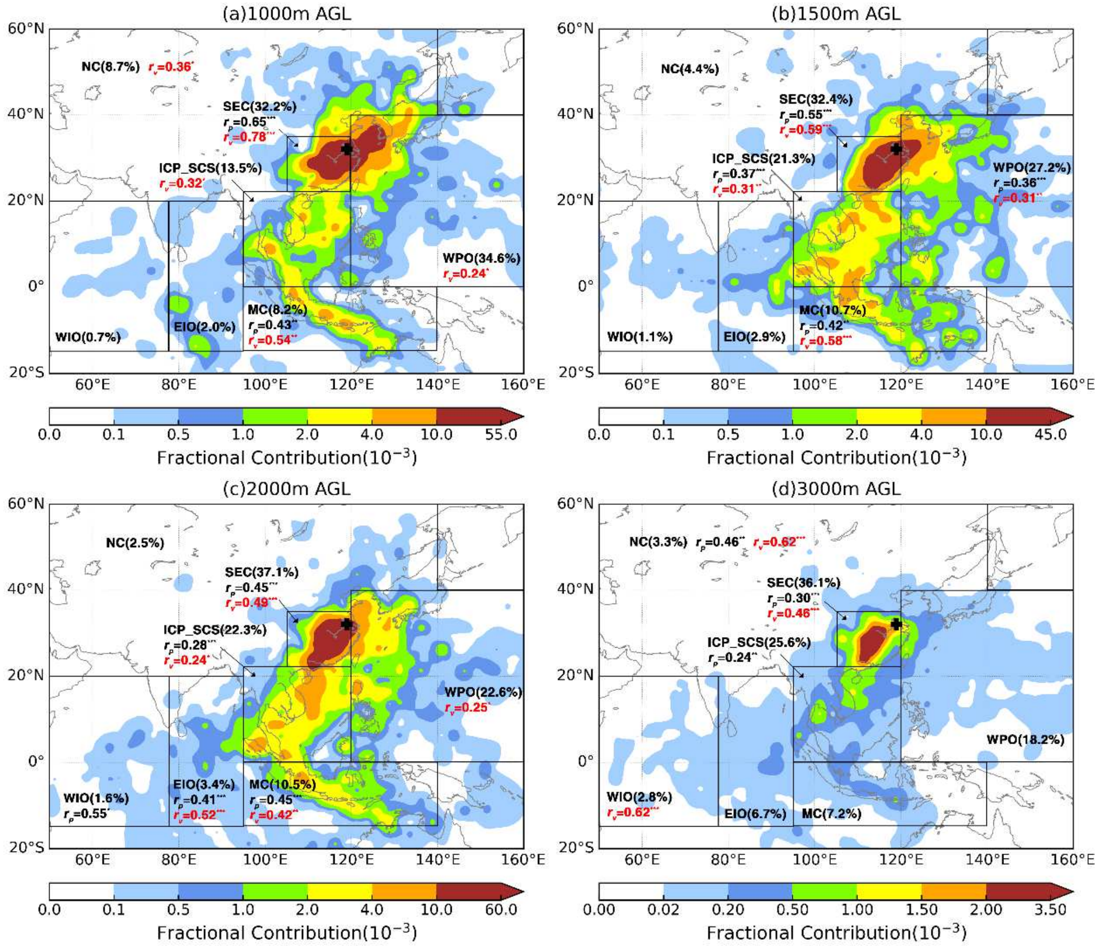

Fig. 4 Fractional moisture contribution (regional summaries in brackets) and correlation coefficients of Nanjing $\delta^{18}O_p$-OLR (r_p, black) and $\delta^{18}O_v$-OLR (r_v, red) in different moisture source regions at initial back-trajectory heights of 1000m (a), 1500m (b), 2000m (c), and 3000m (d) AGL. The black solid line rectangles represent seven moisture source regions. The study site of Nanjing is marked by a black cross. The shading represents the fractional moisture contribution (‰) of individual moisture uptake grid cells for summer precipitation in Nanjing.

Supplementary Files

This is a list of supplementary files associated with this preprint. Click to download.

- SupplementaryInformation1.pdf
- SupplementaryInformation3.xlsx
- SupplementaryInformation2.pdf